Repetition of the Void Space Structure of Achimov Sandstones of the East Urengoyskoye Field in Artificially Created Geometry of a Silicon Microfluidic Chip

M.R. Latypova[1,2], D.I. Pereponov[1,3], V.V. Kazaku[1,3], A. Scerbacova[4], I.G. Maryasev[5], R.A. Mukhin[5], E.D. Shilov[1,3], A.N. Cheremisin[1,3], V.L. Kosorukov[2], V.V. Churkina[2], M.A. Tarkhov[6], V.A. Shtinov[7], T.E. Nigmatullin[7], E.S. Batyrshin[7], I.V. Samsonov[8]*

[1]*LABADVANCE LLC, Moscow, Russian Federation*
[2]*Lomonosov Moscow State University, Moscow, Russian Federation*
[3]*Skolkovo Institute of Science and Technology, Moscow, Russian Federation*
[4]*King Fahd University of Petroleum and Minerals, Dhahran, Saudi Arabia*
[5]*Systems for Microscopy and Analysis LLC, Moscow, Russian Federation*
[6]*Institute of Nanotechnology of Microelectronics of the Russian Academy of Sciences, Moscow, Russian Federation*
[7]*RN-BashNIPIneft LLC, Ufa, Russian Federation*
[8]*ROSPAN INTERNATIONAL JSC, Novyy Urengoy, Russian Federation*

In this work, a unique technique for replicating the void structure of a low-permeability reservoir in a silicon microfluidic chip has been developed. This technique is qualitatively superior to all previous ones and ensures full reproducibility of key parameters of the void structure (permeability; pore size distribution; average channel diameter; channel tortuosity, macro- to microporosity ratio) from digital core data. Moreover, the developed approach enables precise replication of pore geometry from micro-CT images of core samples directly into the microfluidic chip. Using this technique, three artificial void space structures were developed for three samples of Achimov sandstones with different permeability (0.38; 2.04 and 9.86 mD).

The mineralogical composition of the prototype samples was determined by a set of lithological and mineralogical studies and a positive correlation between the intensity of carbonate cementation and the decrease in permeability was revealed. Most of the macropores in the studied sandstones are associated with leaching of feldspars, and micropores are confined mainly to clay minerals. The conducted set of studies on the present samples will facilitate extrapolation of future coreflooding test results to rocks with similar mineralogical characteristics and filtration-capacitance properties.

A qualitatively new method for creating inhomogeneous wettability of artificially created void space structure inside the microfluidic chip was developed. This technique consists in a smooth displacement of formation water from the microchip structure by a hydrophobic agent, which modifies wettability on the surface of macropores and channels, but does not enter the micropore structure due to residual water, which is held inside the microporous structures by capillary forces.

Thus, this work is the first to apply a comprehensive multidisciplinary approach to replicate the core void structure within a microfluidic chip. In the future, this technique will be improved so that the results of coreflooding tests on microfluidic chips will even more reliably reflect fluid movement within the reservoir.

Keywords: microfluidic chip, tight-gas reservoir, Achimov formation, filtration-capacity properties, artificially created void space structure, digital core, lithological and mineralogical complex of studies, inhomogeneous wettability, wettability modification

*Corresponding author: Margarita R. Latypova
e-mail: latypova@labadvance.net

Introduction

The development of hard-to-recover hydrocarbon (HC) reserves is a vital and promising direction in petroleum geology. The greatest interest lies in less explored regions with limited drilling activity, such as the northern areas of the West Siberian Plate (Gydan, Yamal, Nadym-Pur, Yenisei-Khatanga, and Pirtaz oil and gas regions). Research is increasingly focused on the the Achimov clinoform complex (Ach5–Ach6 layers) of the Early Valanginian age (K1v1), which lies above the Bazhenov horizon or the sub-Achimov formation (Decision..., 1991). Despite the promising potential for development, these deposits are considered low-permeability reservoirs due to the deep-water conditions of the Achimov clinoform complex formation and the significant depths at which the productive layers are found (Kurchikov et al., 2013). Hydraulic fracturing is almost always employed for the commercial development of such deposits (Panikarovsky et al., 2020). Additionally, Achimov formation reservoirs in the northern regions of the West Siberian Plate exhibit abnormally high formation pressures and frequent oil-water contact breakthrough (Kuznetsov et al., 2017), complicating HC deposit development and necessitating specialized techniques for isolating water inflows by creating a blocking screen to prevent water migration while maintaining the filtration characteristics of HC-saturated areas.

To carry out these complex procedures in oil and gas field development, preliminary filtration experiments on core samples are essential for selecting the appropriate chemical composition of reagents and determining the optimal conditions for all planned operations. A major challenge of such experiments is their high cost and the fact that a single sample cannot be used for multiple sequential coreflooding tests. Core material often disintegrates after exposure to various solutions and reagents, necessitating the replacement of samples and preventing full repeatability of results. To address this issue, it is logical to replace the pore space structure (PSS) of real core samples with an analogous artificially created geometry within a silicon-glass microfluidic chip.

A microchip is a composite device that contains a specific porous medium. Such PSS can be represented by simple channels or structures that mimic the properties of real core samples. A complex network of microfluidic channels is used to optimize the parameters for modeling a two-phase immiscible flow in a porous system, which is sufficiently complex for observing flow behavior yet relatively simple for determining the exact channel geometry needed to construct a 3D model.

Coreflooding tests using silicon-glass microfluidic chips is currently well-known through several Russian (Pereponov et al., 2023; Scerbacova et al., 2023; Dorhjie et al., 2024) and international studies (Lifton, 2016; Lei et al., 2022). Among these, works focused on designing pore space geometry in a silicon microfluidic chip based on comprehensive lithological-mineralogical studies of the prototype rock sample are noteworthy (Gunde et al., 2010, 2011). These studies consider key PSS parameters, such as pore size and geometry, channel thickness, length, and tortuosity, as derivatives of the encompassing mineral matrix. The ratio of lithological-mineralogical characteristics of the rock to its PSS, as determined by micro-computed tomography (MCT) (Bera et al., 2011, 2012), always plays a crucial role in these studies.

Another important aspect in evaluating the relevance of current research is the potential to extend microfluidic experiments to deposits with similar flow properties (FP). Eventually, after a series of successful coreflooding tests on microfluidic chips, the question arises as to whether the results can be applied to deposits in adjacent fields. The similarity of FP values obtained through flow measurements by the gas volumetric method is insufficient, as this method provides only porosity and permeability data, without any information on pore space morphology. Therefore, obtaining additional information requires costly MCT studies to construct a three-dimensional PSS map of samples from adjacent fields. According to the authors, this additional step can be avoided by thoroughly studying the lithological-mineralogical properties of the prototype samples, as the mineral matrix itself is the key factor controlling the pore space morphology of the rock.

Therefore, the aim of this study is to accurately recreate the PSS of low-permeability Achimov sandstones within a microfluidic chip for further complex multiphase coreflooding tests. Additionally, it is necessary to identify the characteristics of the mineral matrix of Achimov sandstones from the Ach5 layer of the East Urengoy field, that significantly influence the PSS of the studied rocks. Ultimately, based on a comprehensive set of conducted studies, a heterogeneous wettability structure that closely resembles reservoir conditions must be created within the artificially generated PSS in the microchip.

Materials and methods

The material for this study consisted of three standard-sized core samples (80 x 40 mm) and supplementary cylindrical mini-cores (10 x 4 mm) from each standard sample of the Ach5 layer of the Achimov formation at the East Urengoy field. From the standard-sized

cylinder, samples were taken for lithological description of petrographic thin sections (analyst V.V. Churkina) and X-ray structural analysis (XRD) of bulk and clay samples (Fig. 1). Micro-CT with Xenon saturation and mineral composition analysis of the sample using a scanning electron microscope (SEM) were performed on mini-core sample.

Research on the mini-cores was conducted at Skolkovo Institute of Science and Technology using a GE Sensing & Inspection Technologies GmbH v|tome|x L240 X-ray CT system (analyst A.I. Morkovkin). To fully capture porosity, imaging was done in two types of contrast: with air-filled pores and with gas contrast (saturation with xenon under pressure of 29 bar). Submicron space imaging was achieved using three-dimensional visualization with FIB/SEM (Focused Ion Beam/Scanning Electron Microscopy) with xenon. The results were used to construct three-dimensional digital models of the pore space, encompassing both micro- and macroporosity. Based on the digital modeling results, flow properties calculations were performed using GeoDict software (analyst V.V. Kazaku).

Thin sections were prepared at Lomonosov Moscow State University using epoxy resin with a cover glass, with a thickness of 0.02 mm. Petrographic thin sections were described and photographed using an Olympus BX53P microscope and an Olympus SZX16 stereomicroscope, purchased within the framework of MSU development program. Preliminary processed samples for XRD analysis were conducted using a Rigaku MiniFlex 600 X-ray diffractometer (analyst V.L. Kosorukov). XRD of the clay fraction was performed on a primary processed, distilled water-suspended sample of <0.001 mm size.

SEM analysis of core samples was carried out at SMA company (analyst R.A. Mukhin). Sample preparation included processing the mini-core fragment on a Struers Labopol-5 polishing-grinding machine. Surface quality control was performed using a Leica DM LB 2 optical microscope. A conductive layer was deposited on the polished surface using an SPI-Module Carbon Coater. Sample examination under the electron microscope utilized a FEI Teneo single-beam analytical system with dual Bruker Xflash 6/30 micro-X-ray spectral energy-dispersive detectors. Automated mineral composition determination and multi-scale surface mapping were performed using Maps-Mineralogy technology. The results were processed using MAPS-3.1 and ESprite-2.1 software.

Contact angle measurements using the sessile drop method (Mittal, 2004) were performed with a Kruss DSA 30S laboratory instrument at Skolkovo Institute of Science and Technology (analyst A. Scerbacova). Water droplets of 4 μL were placed on the sample surface, and the contact angle of several droplets on the core surface was measured immediately after droplet formation and after 10 seconds of spreading.

The generation of porous media for the silicon microchip was based on digital modeling results from MCT data (analyst D.I. Pereponov). Contours of pores were read and recorded into a separate database from a set of MCT images. This created a dataset with pores sorted by size, including both macro- and micropores. Connectivity between pores was established using watershed segmentation. The methodology for generating the artificially created porous structure is detailed in the «Results» section.

Microfluidic silicon chips with glass covers were fabricated at the Institute of Nanotechnology of Microelectronics of the Russian Academy of Sciences under the supervision of M.A. Tarkhov. The fabrication process resembles standard microelectronics industry procedures. Initially, the silicon substrate was cleaned using hydrodynamic technology. A 2 μm-thick photoresist (PR) layer was then applied, with hexamethyldisiloxane used for improved adhesion. The microchannel pattern was created using laser lithography, followed by PR development in an aqueous potassium
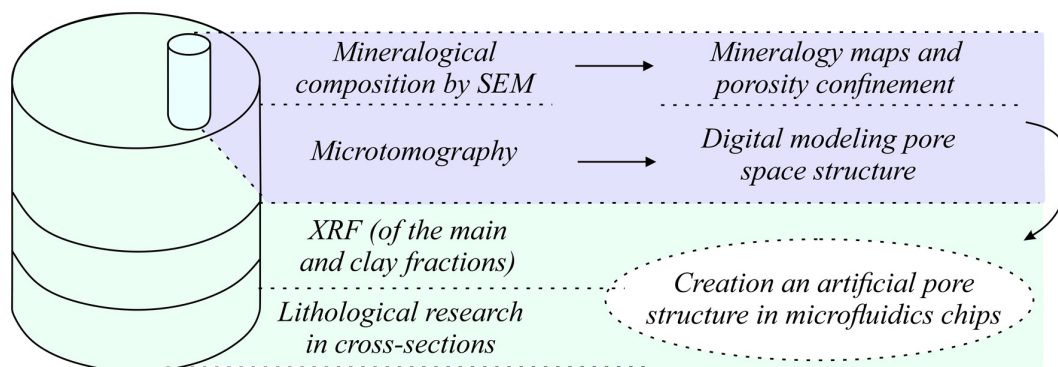

Fig. 1. General complex of studies of the standard core sample of the Achimov sandstone and its mini-core (fragment of the standard cylindrical sample)

Repetition of the void space structure of Achimov sandstones…   M.R. Latypova, D.I. Pereponov, V.V. Kazaku et al.

gr⋀⋀

www.geors.ru

hydroxide solution. Bosch technology was used for deep anisotropic silicon etching to the desired depth. Post-etching, residual protective passivation layers and PR were removed in oxygen plasma. Through-channels for liquid input/output were created using laser ablation. The final step was anodic bonding of the silicon wafer with borosilicate glass.

Hydrophobization of macropores in the artificially created porous structure in the silicon-glass microchip was achieved by initially injecting synthetic brine into the microfluidic chip, followed by its displacement with a hydrophobizing solution that was left for imbibition for 4 hours. Stearic acid 98.5% (Sigma), dissolved in decane (acid concentration 0.01 mol/L or 2.8448 g/L), was used as the hydrophobizing agent. To evaluate the degree of brine displacement by stearic acid, aqueous phase was dyed with a fluorescent dye to clearly differentiate the phases under a fluorescent microscope. Thus, through two-stage injection into the artificially created structure of the microfluidic chip, heterogeneous wettability characteristic of gas condensate sandstone reservoirs was simulated.

Results
MCT of mini-core samples, construction of digital models

Based on the results of the conducted MCT studies, three digital models of mini-core samples from the Ach5 reservoir layer were constructed. These models aimed to obtain representative numerical characteristics of pore space morphometry and flow properties for designing microfluidic twin chips with three different permeability coefficients (Kp): 0.38, 2.04, and 9.86 mD (Fig. 2). For each model, the key parameters characterizing pore space were determined, namely:

1. Permeability (Fig. 2a);
2. Porosity (Fig. 2b);
3. Tortuosity (Fig. 2c);
4. Aspect ratio of pores (Fig. 2d);
5. Volumetric fraction of pore channels (Fig. 2e) and pores (Fig. 2f), specifically the distribution of channels and pores by size.

Digital modeling results revealed that all three samples have different porosity and permeability. The most significant differences are in Kp, which ranges from 0.38 mD in the lowest permeability sample to 9.86 mD in the highest permeability sample. Porosity values also vary but to a minor extent (5.35–9.86%).

Tortuosity of channels, defined as deviation of the actual path length of the fluid flow from the length of the rock sample (Romm, 1985), varies slightly among the three samples (from 1.2 to 1.8). The pore aspect ratio, which is the ratio of pore diameter to pore channel diameter, also shows minor variations across the three samples. Additionally, the volumetric fraction of pores and pore channels is similar for all three samples. On average, the diameter of the pore channel ranges from 5 to 10 μm, and the average pore diameter varies from 15 to 20 μm. Thus, it was determined that among all calculated pore space characteristics, Kp shows the most significant variation across the three samples.

Microfluidic chip structure generation

Geometry of pore space within the silicon microfluidic chip was developed based on digital core data of the prototype rock. The process of creating the microfluidic chip geometry can be divided into the following stages:
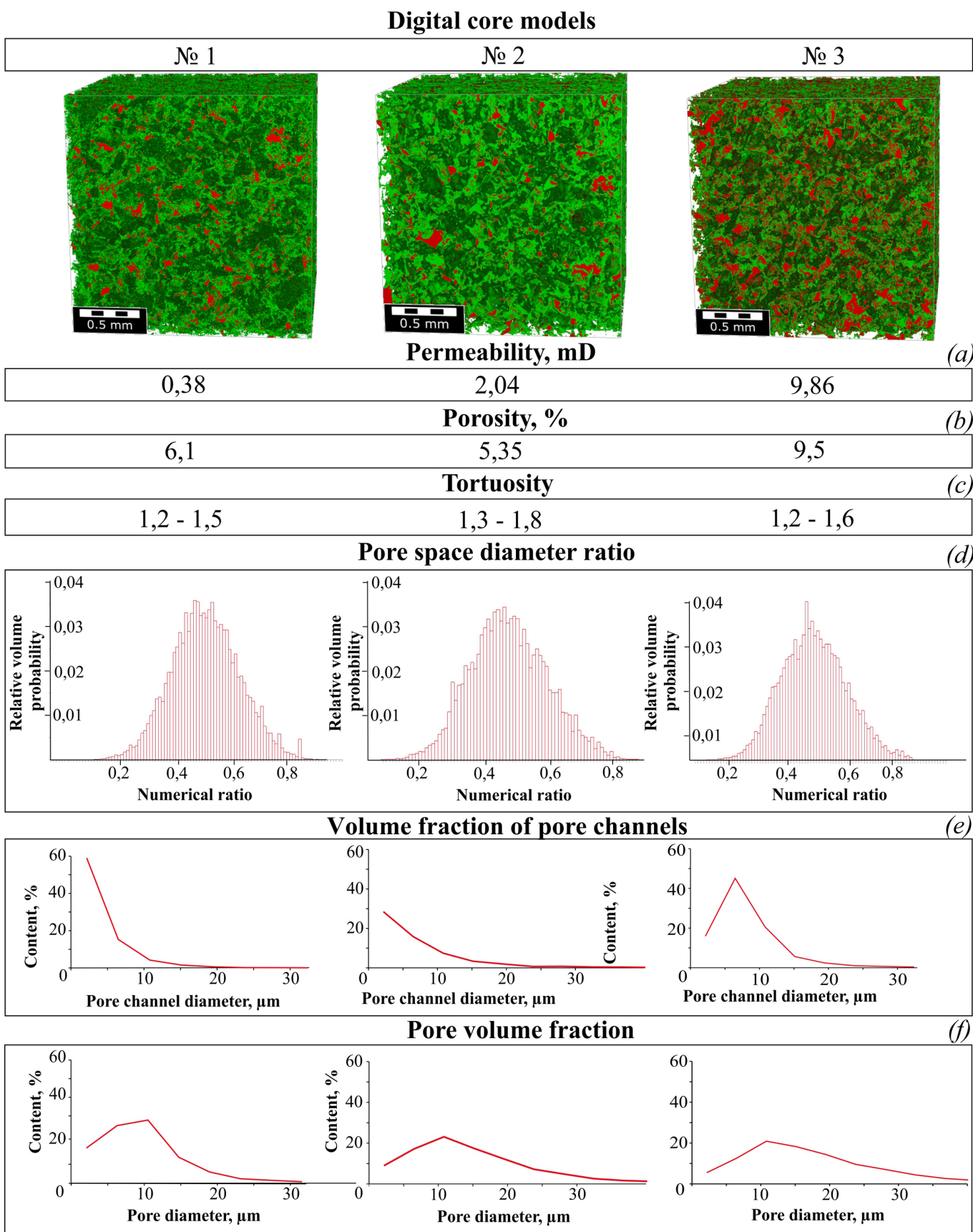
1. Initially, the cube of the digital model (Fig. 2) is converted into a set of black-and-white images. In each binarized image (over 1000 layers) (Fig. 3a), pore contours were delineated using specialized software (Fig. 3b), each of which was stored in a unified data array. It is worth noting that each macropore was stored in this array along with its adjacent microporosity.

2. The next step involves processing of the created data array containing information about the pore geometry. In each pore of irregular geometry stored in the array, a group of maximum-radius circles is inscribed (Fig. 3c), allowing the pores in the dataset to be sorted by diameter. Each pore is stored in the data array along with information on the number and size of the inscribed circles.

3. The following step involves transferring the sorted pores, based on size, onto a standard-sized mask. The reference pore size ratio is derived from the digital modeling results (Fig. 3d). The resulting image reflects the actual pore size distribution; however, all pores remain unconnected (Fig. 3d).

4. To add connectivity to the artificially created geometry, watershed segmentation is used. This process identifies image contours based on regions with the highest absolute gradient value (Beucher, Lantuejoul, 1979). The image is represented as a geomorphological map with peaks and local minima (Fig. 3e1). Various algorithms for watershed transformation are described in past literature (Beucher, 1991; Beucher, Meyer, 1993). In this case, watershed segmentation is applied to identify the space between pores, with size of these areas controlled by blurring parameters (Fig. 3e2).

After creating the channels, their width and etching depth were chosen to match the average pore channel diameter from the digital modeling data.

Fig. 2. Results of digital modeling of three studied samples according to GeoDict data with calculated values of porosity, permeability, ratios of diameters of pore spaces, volume fractions of pores and pore channels
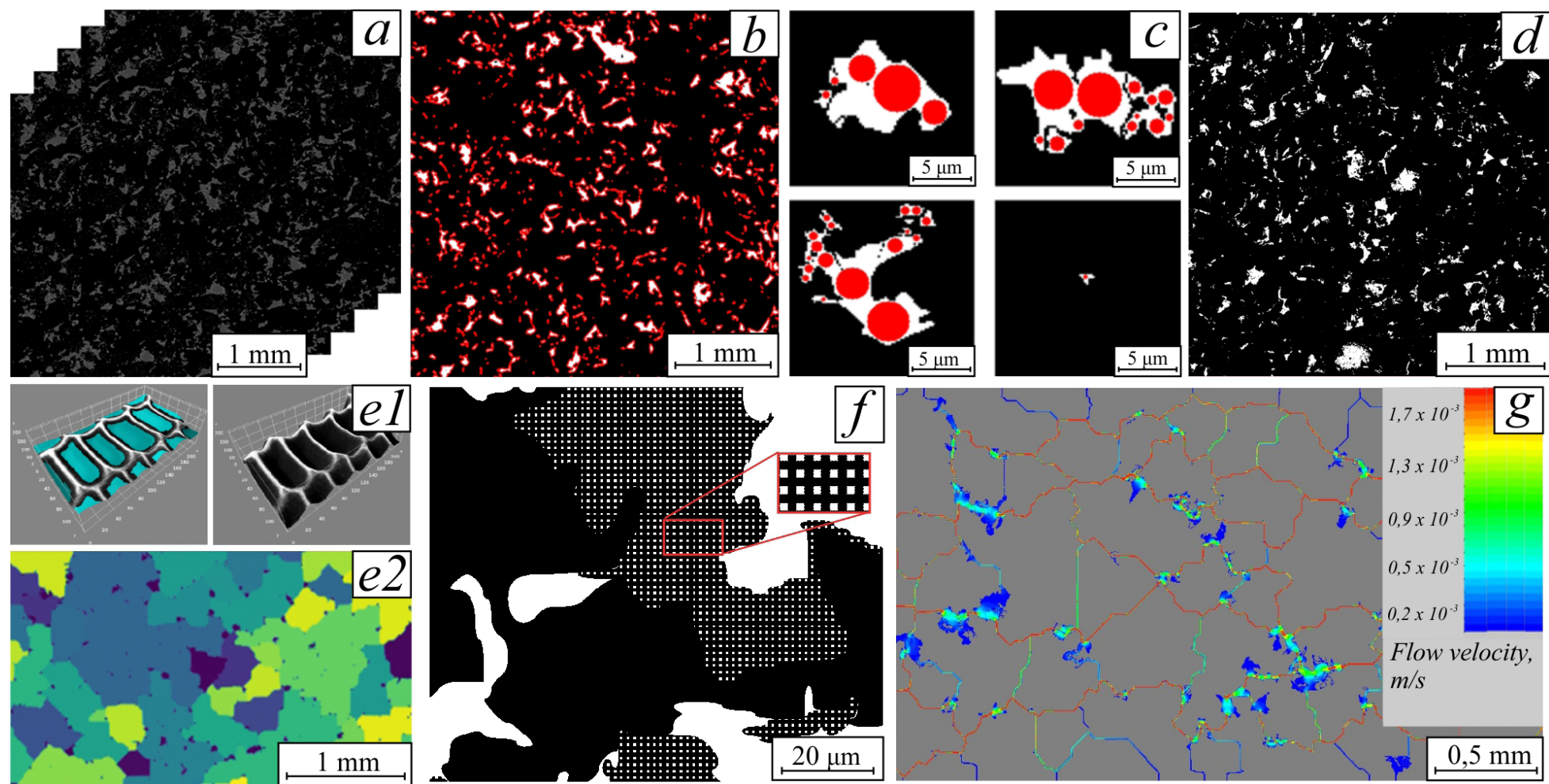
Fig. 3. Stages of creating the artificial geometry of a microfluidic chip based on the digital model of actual Achimov sandstone cores (a - binarized CT images; b - extracted pore contours on the binarized CT image; c - circles inscribed within complex geometry pores; d - pores transferred onto a standard-sized mask; e1 - visualization of watershed segmentation; e2 - mask with transferred pores after applying watershed segmentation; f - Fragment of the created geometry with macro- (black) and microporosity (grid); g - flow velocity distribution field for the developed geometry in GeoDict software.

5. As mentioned earlier, the artificial geometry of the microfluidic chip includes both macro- and microporosity. Describing such small-scale zones is a non-trivial task, so it was decided to represent the microporosity as a grid of elements 0.8 by 0.8 µm (Fig. 3f). For micropores, a different etching depth of the silicon plate will be selected in further work to preserve their micron-scale size in the microfluidic twin.

6. The final step involves calculating the resulting Kp in GeoDict simulator to compare it with digital modeling results. The Kp value was obtained by simulating the injection process of the HC phase through the artificially created porous structure (Fig. 3g). If the permeability of the artificial geometry did not match the digital modeling results, the geometry was modified accordingly. Ultimately, after several iterations, the desired flow parameters were achieved.

Following the above-described procedure, artificial geometries for microfluidic chips were designed based on three digital models with different permeability coefficients: 0.38, 2.04, and 9.86 mD. Subsequently, microfluidic chips with the dimensions of 4×1.2 cm were manufactured with the generated geometries incorporated in micromodels. The size of the artificially designed geometry with etched pores and channels was 2×6 mm. Figure 4 presents photographs of the fabricated microfluidic chips.

Lithological description of petrographic sections

In thin sections, all three samples are represented by fine- to very fine-grained (0.01–0.5 mm) polymictic sandstones, well-sorted, with an admixture of silt-sized (7–10%) and medium sand-sized (10%) material, exhibiting good sorting and mechanical conformity of fragments (Fig. 5).

The sandstones consist of angular to subangular, occasionally angular, quartz grains (30–35%), feldspars (55–60%), lithic fragments (3%) from metamorphic, sedimentary, and igneous rocks, with mica flakes (7%) present in the mineral matrix. The shape of plastic fragments (micas, slates) indicates structures of gravitational compaction – a mechanical process that alters the shape of soft fragments under lithostatic pressure. The orientation of mica flakes creates indistinct cross-bedding. Fragment relationships are primarily mechanically conforming and rarely linear. Cement is predominantly chloritic, occasionally pore-filling fine to very fine crystalline calcitic (up to 3%), with localized regenerative quartz cement, and mainly cementation by pressure solution. Secondary alterations include
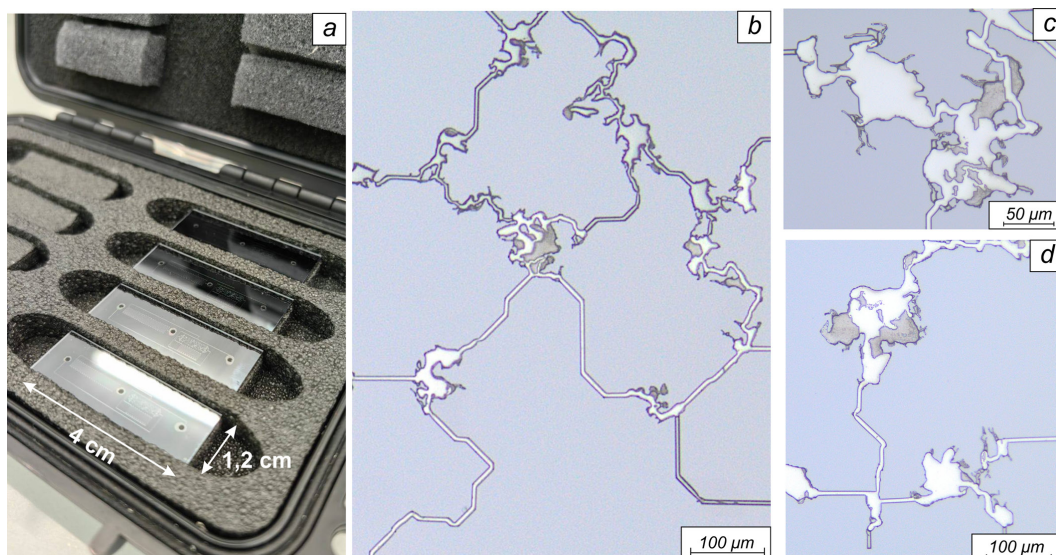

Fig. 4. Photographs of manufactured microfluidic chips (a) using artificially created geometries, photographs of fragments of void space under an optical microscope (b-d) with macro- (white) and microporosity (gray) at different magnifications
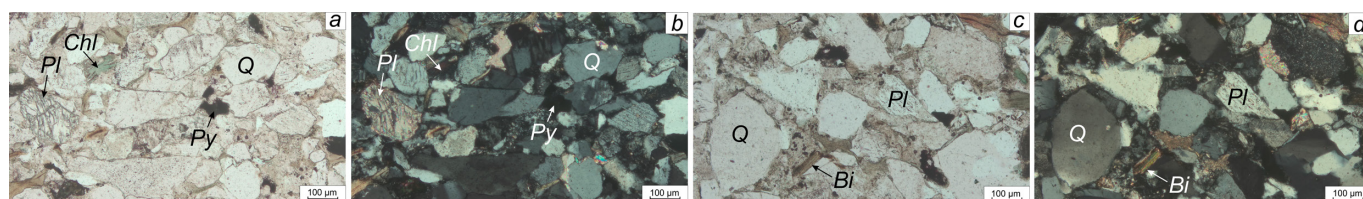

Fig. 5. Photographs of petrographic thin sections in // (a, c) and X (b, d) nicols from the studied samples of the Achimov Formation. Mineral constituents in the thin sections: Q – quartz; Pl – plagioclase; Py – pyrite; Chl – chlorite; Bi – biotite

Repetition of the void space structure of Achimov sandstones…   M.R. Latypova, D.I. Pereponov, V.V. Kazaku et al.

gr /\^/\
www.geors.ru

early iron oxides and pyrite (1%), primarily associated with organic matter and replacing individual fragments. Almost all primary pore space in the studied rocks is filled with secondary quartz overgrowth (Fig. 6e) and chloritization.

The feldspars (55–60%) are represented by potassium feldspar (K-feldspar) and plagioclase. K-feldspar includes microclines and orthoclases, angular to subangular, tabular grains, secondarily pelitized. Plagioclase consists of semi-rounded fragments with polysynthetic twinning according to the albite law, oligoclase composition, and locally secondarily sericitized (Fig. 6a). Myrmekites that are worm-like intergrowths of quartz in oligoclase are noted (Fig. 6b). Occasionally, more basic plagioclases of the oligoclase-andesine series are found. Some plagioclases are albitized (Fig. 6c) or along the grain edges. In some places, feldspars are partially dissolved with empty or kaolinite-filled pores (Fig. 6d), and in other areas, feldspars are completely dissolved.

Mineralogical composition according to RSA data

Mineralogical composition of the three samples, based on X-ray diffraction analysis of bulk (Fig. 7) and clay samples, is also almost identical. The bulk samples are predominantly composed of plagioclase grains (38–41%), quartz (27–33%), and potassium feldspar (15–19%). Chlorite within mineral grains (chloritization of feldspar) (7–10%) and micas (4–5%) have subordinate significance. Among the clay fraction, chlorite predominates (82–91%), with micas (5–12%) and other mineral compounds (quartz and feldspar 4–6%) being less significant.

Mineralogical composition according to SEM data

Mineral distribution maps, built based on SEM analysis of mini-core samples, did not reveal substantial differences in the mineralogical composition of mini-core samples, that were used to construct digital rock models based on micro-CT data. In addition, the mini-cores have a mineral composition that is nearly identical to that of standard cylindrical samples from the studied formation.

Plagioclase (35–39%), quartz (24–27%), and potassium feldspar (8–10%) dominate the mineral matrix structure (Fig. 8). The main clay mineral is chlorite (8–10%), and micaceous minerals, including biotite and muscovite, account for approximately 6% of the entire mineral matrix. Accessory minerals include garnet, illite, rutile, and apatite. The proportion of secondary calcitization is extremely low (1–2.1%).

Notably, the highest permeability sample (9.86 mD), Sample No. 3, has the lowest content of pore-filling calcite (1%), whereas the lowest permeability sample (0.38 mD), Sample No. 1, contains more than twice as much calcite and still represents only a small fraction of the total mineral matrix (2.1%).

High-resolution electron microscopy of the core samples revealed that majority of macropores identified by micro-CT result from the secondary leaching of plagioclase grains (Fig. 9). Most microporosity is associated with the clay chlorite cement. Primary porosity, due to the intense secondary alteration of the sandstones, has been almost entirely replaced by secondary quartz overgrowths.
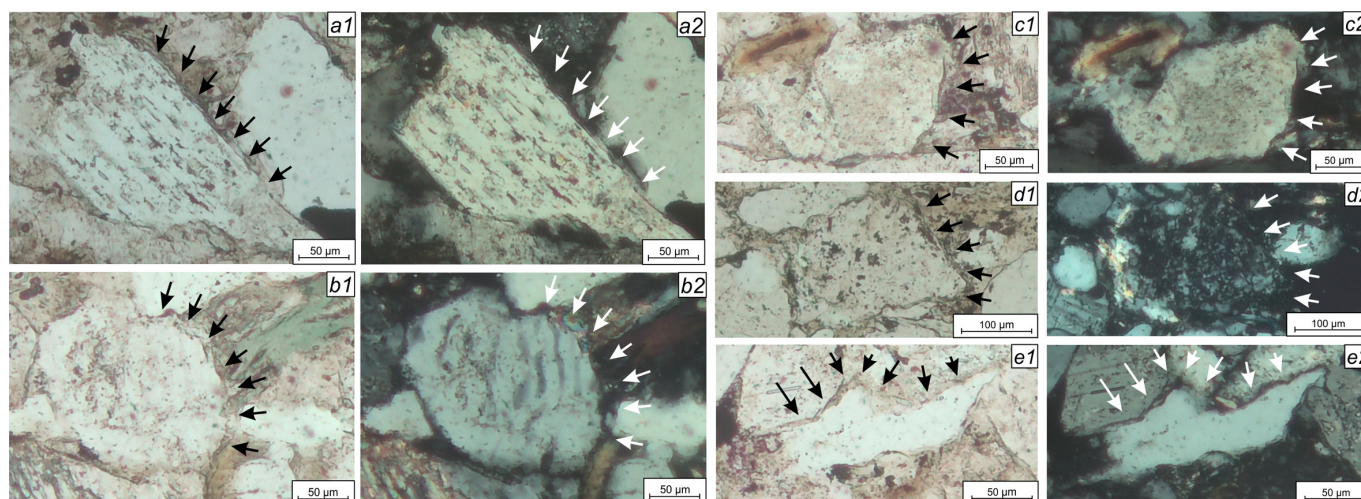

Fig. 6. Photographs of the most common secondary alterations in quartz and feldspar grains of the sandstone in thin sections in // (1) and X (2) nicols: a – sericitization of plagioclase; b – quartz myrmekites in plagioclase; c – pelitization of feldspar; d – kaolinitization of feldspar; e – secondary quartz overgrowth (quartz regeneration)
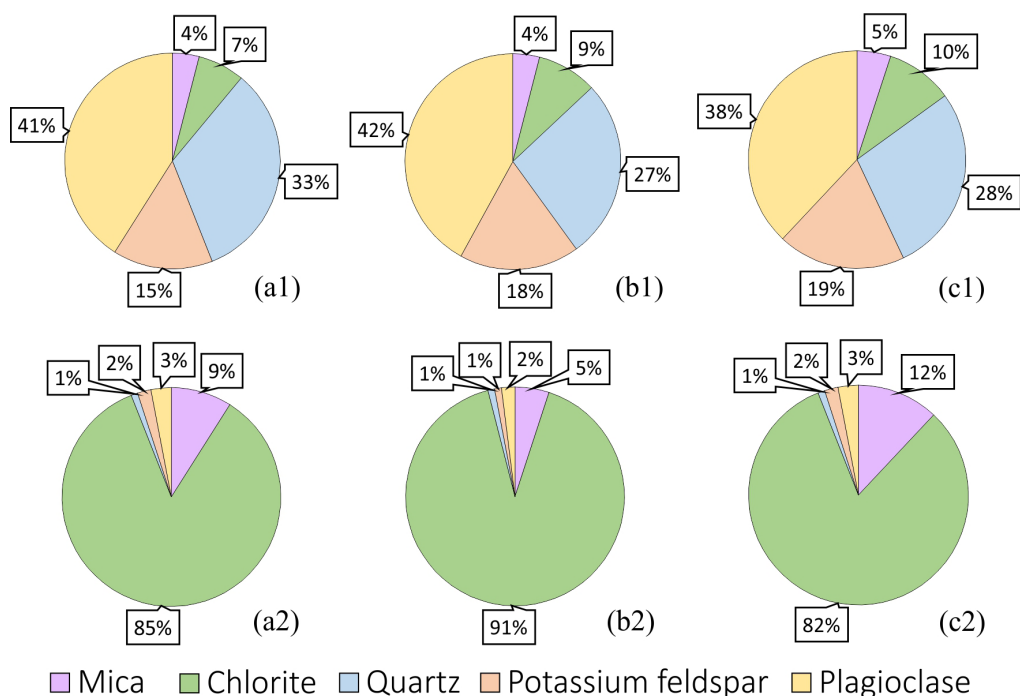
Fig. 7. Histograms showing the percentage of mineral components based on X-ray diffraction (XRD) analysis of bulk (1) and clay (2) samples from the studied specimens (a, b, c)
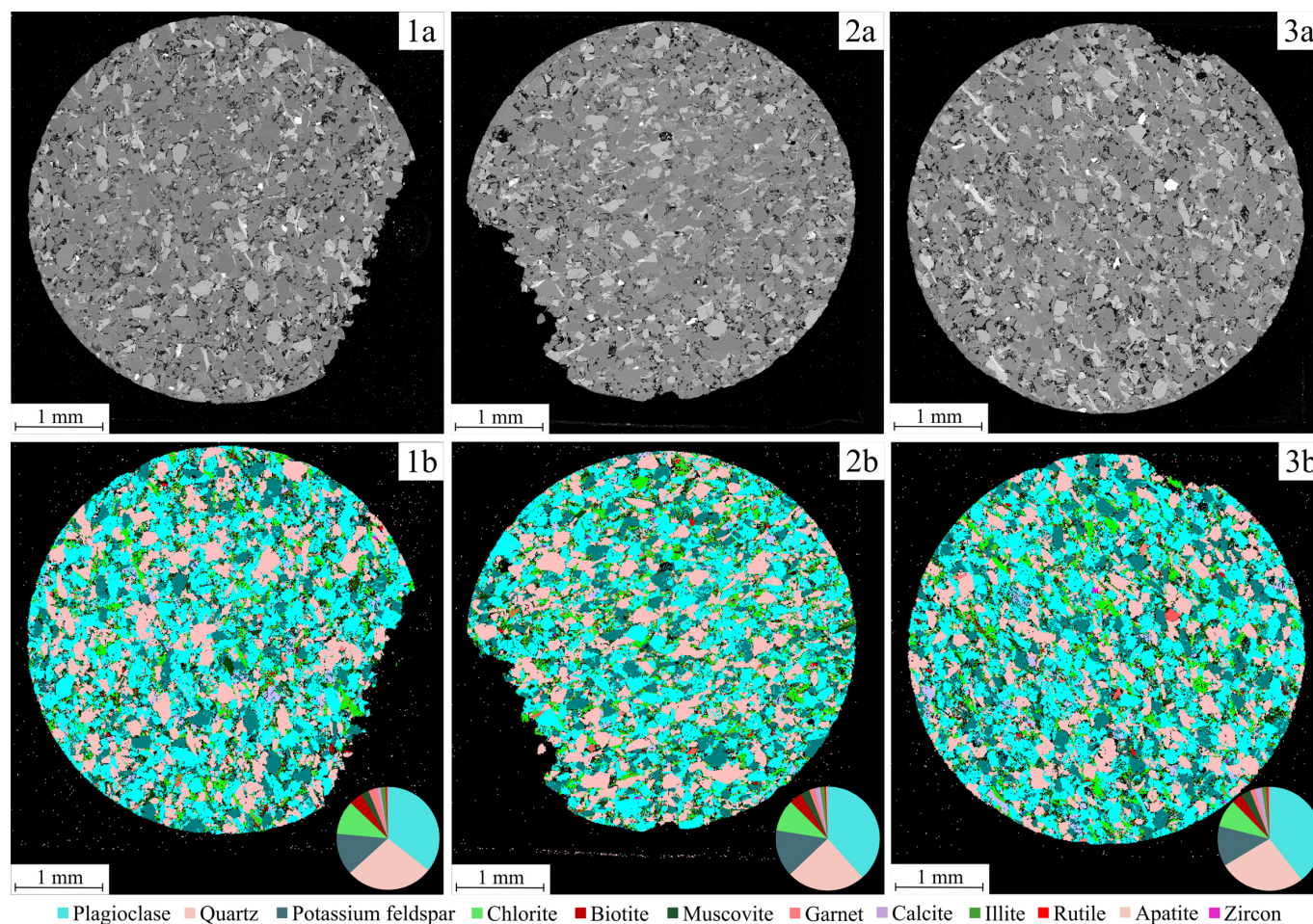

Fig. 8. Surface area maps (a) and mineral distribution maps with pie charts of mineral composition (b) for the studied samples of mini-cores (1, 2, 3) with different permeability ranges according to digital modeling data

Repetition of the void space structure of Achimov sandstones…   M.R. Latypova, D.I. Pereponov, V.V. Kazaku et al.
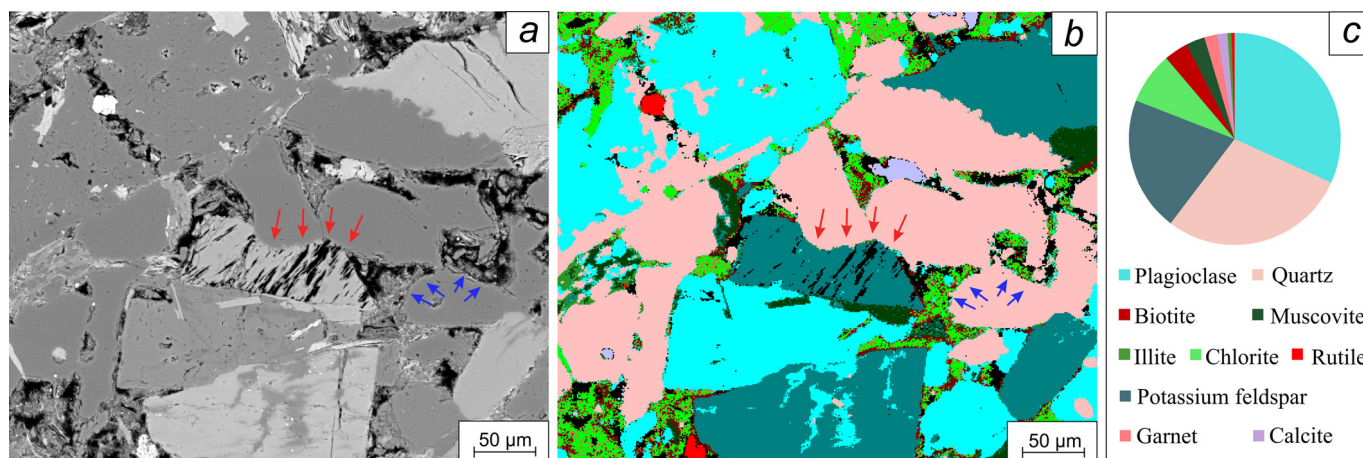
gr /\/\
www.geors.ru

Fig. 9. Surface area maps (a) and mineral distribution maps with pie charts of mineral composition (b) for the studied samples of mini-cores (1, 2, 3) with different permeability ranges according to digital modeling data

Contact angle measurements

To closely replicate physicochemical properties of natural rock on a silicon-glass microfluidic chip, it is crucial to consider wettability that significantly impacts fluid distibution and propagation. To accurately modify the wettability of silicon substrate and, consequently, the modeled microporous medium, it is essential to assess the properties of the material used. Therefore, to create heterogeneous or selective wettability (Salathiel, 1973) on the silicon surface of microfluidic chip before bonding it with glass, a preliminary investigation of water contact angle of the prototype core was conducted.

Water contact angles captured immediately after being placed on rock surfac range from 42° to 60° (Table 1). After 10 seconds of spreading, the contact angle decreased to 26°–37°. For all three samples with different permeabilities, the contact angle values were identical, confirming the hydrophilic nature of the samples. However, it should be noted that wettability was investigated after chloroform extraction of the cores/plugs, which eliminates the influence of hydrophobic components on the surface of the studied samples. The natural hydrocarbon compounds were artificially

removed, so the results do not reflect the actual heterogeneous wettability in the reservoir.

Similar contact angle measurements on the silicon substrate surface showed results comparable to those of the prototype core, indicating that the silicon substrate used for microfluidic chips is predominantly hydrophilic.

Discussion

Comparison of prototype cores and microfluidic chips

Comparison of digital model with microfluidic chips demonstrated significant convergence in the characteristics of artificial porous structure within the chip, as compared to the parameters of the prototype rock (Table 2). Since the pore geometry was replicated from MCT images, it is expected that this parameter is fully convergent between the rock and artificially generated structure. There is notable convergence in the permeability values (Kp) between the prototype sample and the microfluidic chip. For instance, for sample 1 with Kp = 0.38 mD, the MCT data, after several iterations of recalculating the mathematical model, generated a porous structure with Kp = 0.61 mD.
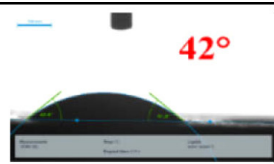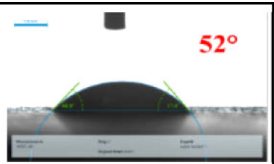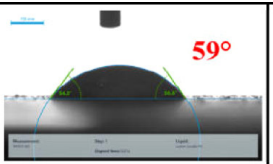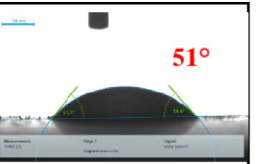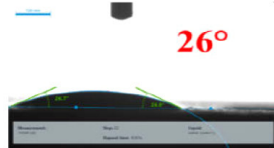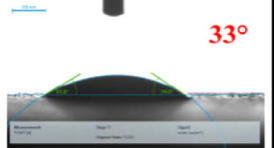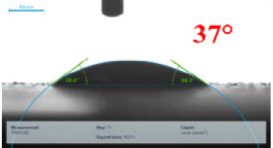
	Water drop			
Water drop after forming	42°	52°	59°	51°
Water drop after 10 seconds of "spreading	26°	33°	37°	36°

Table 1. Contact angle of water droplets on the core surface of Achimov sandstones

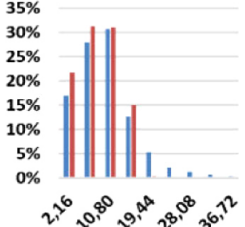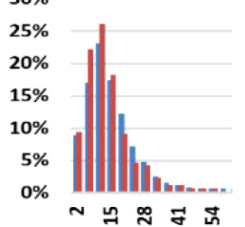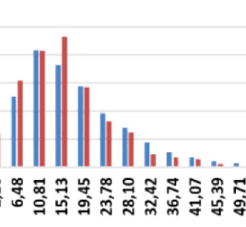| Sample number	1		2		3	
Digital model/ microchip	Digital model	Microchip	Digital model	Microchip	Digital model	Microchip
Permeability (mD)	0,38	0,61	2,04	3,43	9,86	12,17
Pore throat distribution (um)	3,36*	3**	5,08	5	7,7	7
Tortuosity	1,2 – 1,5	1,35	1,3 – 1,8	1,33	1,2 – 1,6	1,31
Pore geometry	Repeated from MCT data					
Pore size distribution (on the y–axis - the number of pores; on the x–axis - the diameter of the pores)						

Table 2. Values of permeability, tortuosity and channel size distribution in core samples and porous structures of microfluidic chips. Note: All parameters were measured in the GeoDict software for three mini-cores of prototypes, and for artificially generated microfluidic porous structure; * – the average diameter of the channels, ** – the same size for all channels; on the histograms of the pore size distribution: blue – pores in the prototype sample according to the MCT data, red – pores on the microfluidic chip

The method developed in this work for porous structures in microchips based on digital modeling is novel and represents a significant improvement over previously proposed techniques.

The most well-known methods for replicating rock structures on microfluidic chips have been based on copying X-ray tomography (Lacey et al., 2017) and SEM (Buchgraber et al., 2011) images. A significant drawback of these approaches is the lack of control over the distribution of pore sizes and channels.

The Pore Network Model, which creates structures using spheres and cylindrical channels (Pradhan et al., 2019), is widely used in microfluidics and allows for the control of pore sizes and quantities. However, it does not capture the true characteristics of the pore space in geological formations, such as channel tortuosity and pore morphology.

All of these parameters were accounted for in this study. Channel tortuosity was replicated from digital modeling data, and pore shapes were precisely copied from CT scan images. Pore size distribution was also accurately replicated from the digital model data.

This new method is suitable for the high-quality design of low-permeability structures, the modeling of which is technically challenging. At the same time, the generation of low-permeability porous media is a promising direction in the study of unconventional hydrocarbon reservoirs as it's development is becoming increasingly relevant.

Influence of the rock mineralogical composition on their filtration properties

It is well-known that the most important parameters that have effect on the petrophysical properties of sandstones are their morphological (grain contact and rounding, cement type), granulometric (grain size, sorting), and mineralogical (mineral composition) characteristics. These are affected by numerous external factors such as sedimentation conditions, secondary transformations, and burial depth of the studied deposits (Scherer, 1987). However, it should be noted that a clear correlation between permeability and lithological composition is not always observed in low-permeability sandstone reservoirs (Rushing et al., 2008). It was found that granulometric and mineralogical compositions of all three studied samples are almost identical. The compositions were defined based on lithological descriptions, SEM images and XRD analysis results. Numerical petrophysical characteristics obtained through digital modeling based on CT scan data also show only minor difference, with the exception of permeability. Thus, for the studied deposits, there is no clear correlation between lithological-mineralogical characteristics and permeability, except for the increased content of pore-filling calcite in the samples with lower Kp. Secondary calcitization that is a widespread process leading to reduced permeability in Achimov deposits is not prevalent within the studied Ach5 interval. However, even minor secondary alterations resulting in slight calcitization (1–2%) in some samples may affect their permeability.

Repetition of the void space structure of Achimov sandstones…   M.R. Latypova, D.I. Pereponov, V.V. Kazaku et al.

gr /\/\

www.geors.ru

It is commonly known that clayey cement in sandstone reservoirs often occupies a significant portion of the intergranular pore space, leading to channel blockage and reduced permeability (Nelson, 2009; Xi et al., 2015). However, not all clay minerals have an equally negative effect to the petrophysical properties of sandstone reservoirs. The studies conducted revealed that the primary clay minerals in the mineral matrix of the investigated samples belong to the chlorite group, suggesting that clay minerals may not significantly impair reservoir properties during exploitation. Furthermore, there is a near-complete absence of hydromica clay minerals in the studied rocks, which could otherwise lead to significant permeability reduction due to "intracrystalline swelling of clay minerals" (Mooney et al., 1952; Morris, Shepperd, 1982).

Entire primary porosity in the studied samples is almost entirely filled due to late diagenetic transformations (secondary quartz overgrowth, kaolinization, sericitization) that is typical of Achimov clinothems. The formation of most secondary pore space in the studied samples is also related to late diagenetic and catagenetic transformations within the most unstable mineral grains, particularly within feldspars. Notably, the majority of macropores in all three studied samples were formed due to feldspar leaching (Figure 10, a, b). XRD results show that feldspar content in the studied sandstones varies from 57% to 60%. Among the secondary transformations of feldspars, sericitization, pelitization, and kaolinization of plagioclases are most prominent. Meanwhile, most microporosity is associated with the structure of clay minerals from the chlorite group (Fig. 10, c, d).

Creation of heterogeneous wettability on a microfluidic chip

Wettability, an important parameter influenced by surface forces, significantly affects the behavior of reservoir fluids (Bartell, Osterhof, 1927). In the context of hydrocarbon reservoir development, the study of rock

wettability became a highly relevant topic in the mid-1960s (Moore, Slobod, 1955; Slobod, Blum, 1952) when it was discovered that the presence of hydrocarbons in a reservoir leads to substantial hydrophobization of rock surface (Amott, 1959). It is now well-established that wettability of a reservoir significantly impacts the effectiveness of most known hydrocarbon extraction technologies, and incorrect assumptions about rock wettability can lead to irreversible damage and complications in reservoir development.

In the pore space of rocks from productive Achimov strata, heterogeneous or selective wettability (mixed-wettability condition) is often observed (Salathiel, 1973). In most cases, heterogeneous wettability in oil reservoirs is explained by hydrocarbons within the reservoir that displace water from the larger connected pores into smaller pores and capillaries. In case of heavy oil reservoir oil chemical composition significantly affects the wettability of the porous surface where the hydrocarbons have been present for an extended period (Johansen, Dunning, 1961; Strassner, 1968). Heavy hydrocarbon compounds can separate from oils and affect the internal surface of the pores (Bobek et al., 1958; Mungan, 1972). Consequently, in oil-saturated reservoirs the large, interconnected pores occupied by hydrocarbons are typically strongly hydrophobized, whereas the surfaces of pores filled with brine remain comparatively hydrophilic.

The studied deposits belong to a gas-condensate reservoir. Consequently, it was decided to account for the heterogeneous wettability of the rock's pore space, with particular attention to the differing wettability of micro- and macropores. The hypothesis is based on the concept that water, held by capillary forces, resides in the smaller pores. Therefore, if the initial wettability of the reservoir is hydrophilic, the smaller (micro-) pores will remain hydrophilic during gas-condensate flow because they are occupied by residual water and cannot be displaced by the condensate. Polymictic arkosic sandstones are inherently hydrophilic, so the only

■ Plagioclase   ■ Quartz   ■ Biotite   ■ Muscovite   ■ Illite   ■ Rutile   ■ Potassium feldspar   ■ Chlorite   ■ Garnet   ■ Calcite
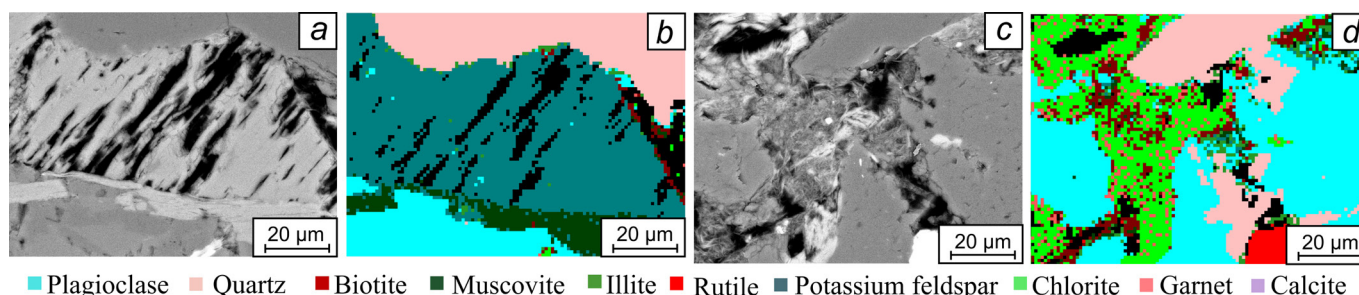
Fig. 10. Fragments of surface areas maps (a, c) and maps of mineral distribution (b, d) according to SEM data with areas of extensively developed macro- (a, b) and microporosity (c, d)

parameter that could influence the hydrophobization of the porous media surface in the studied rocks are the hydrocarbons present in the reservoir.

During flow, the gas condensate will occupy the larger pores and displace the gas that was initially present in these pores. Thus, the larger pores will be hydrophobized to some extent. It was decided to hydrophobize the larger pores and their connecting channels (macroporosity), to a minor degree in order to ensure that the overall model remains predominantly hydrophilic. The wettability of the silicon substrate around the microporosity remained unchanged (hydrophilic). A schematic representation of the micromodel with mixed wettability is shown in Figure 11. The average contact angle was 75°.

Several methods for wettability modification of silicon wafer surfaces are well established in the literature:

1. Silanization of the silicon surface. It involves treating the silicon surface with organosilicon compounds known as organosilanes. The process of silanizing a silicon wafer surface with TCP-silane solution in 96% ethanol is described by N.K. Karadimitriou (2013). By varying the concentration of organosilane, different contact angles on the treated surface were achieved. However, this method has drawbacks, including uneven hydrophobization and the formation of "flakes" in the micromodel due to the reaction between organosilane and water, and these flakes can block micropores.
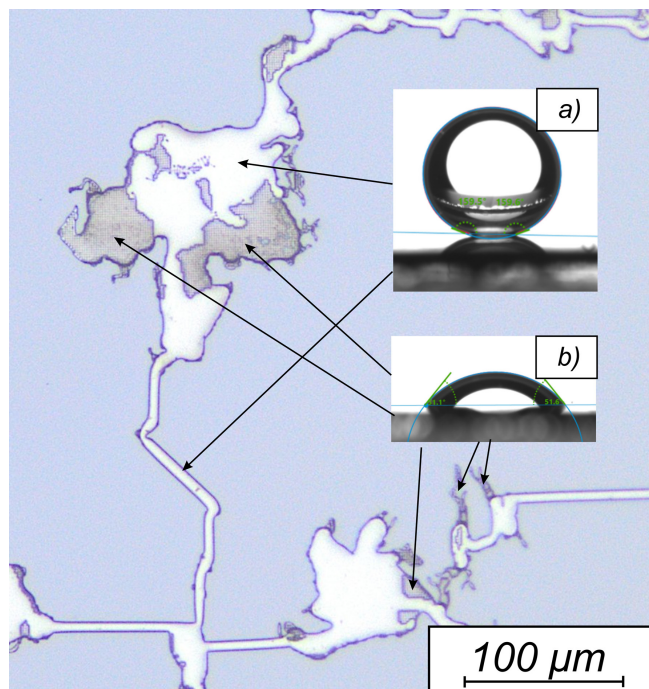

Fig. 11. Schematic distribution of inhomogeneous wettability for micro- and macropores in a microfluidic chip, where the macroporosity and channels are hydrophobic (a), and the microporosity remains hydrophilic (b)

Prolonged exposure to organosilane may also lead to partial corrosion of the chip, consequently increasing the permeability of artificially created porous structure.

2. Piranha solution treatment. This method involves treatment of the surface with a mixture of sulfuric acid (H_2SO_4) and hydrogen peroxide (H_2O_2). K.S. Koh et al. (2012) used various acids and H_2O_2 to create a more hydrophilic surface. Treatment with this solution results in the formation of a 1.3 nm thick amorphous coating on the silicon surface (Li et al., 2023), enhancing the surface hydrophilicity. However, a limitation of this method is its tendency to alter the surface structure, including inducing 'swelling' upon reaction with decane (Koh et al., 2012).

3. Electrochemical manipulation of oxidation states. The procedure involves controlling the wettability of a copper surface ($CuO + Cu_2O$) by altering its oxidation state (Zahiri et al., 2017). This approach can be applied to a microfluidic chip by thin layer deposition of copper on the surface of the pre-etched porous structure before bonding the microfluidic chip to glass. However, this method is complex in implementation and requires careful preparation and specialized equipment.

4. Aging the surface with stearic acid. The method involves treating the surface with acid solution, which roughens the silicon wafer surface and thereby increases the contact area of a droplet with the surface (Iglauer et al., 2020; Ali et al., 2021). The mechanism for modifying wettability that we have developed is described in the Materials and Methods section.

Figure 12 illustrates three phases of fluid injection to achieve heterogeneous wettability of the porous structure in a microfluidic chip. During the injection of hydrophobizing agent at a low differential pressure, some water retained within the micropore structure was not displaced by the hydrophobizing solution due to capillary forces and thus was not subjected to hydrophobization (Fig. 12, c). Consequently, heterogeneous wettability was established/achieved within the porous structure of microfluidic chip that is typical for Achimov reservoirs in gas-condensate fields.

Conslusion

The conducted research resulted in the following significant findings.

1. A new and unique methodology for artificial porous structure design based on CT data of core samples has been developed. This method is innovative and qualitatively surpasses previously proposed approaches. The developed technique ensures nearly complete reproducibility of several key parameters of the core porous structure in the silicon microfluidic chip,

Repetition of the void space structure of Achimov sandstones…   gr⁄⩕   M.R. Latypova, D.I. Pereponov, V.V. Kazaku et al.
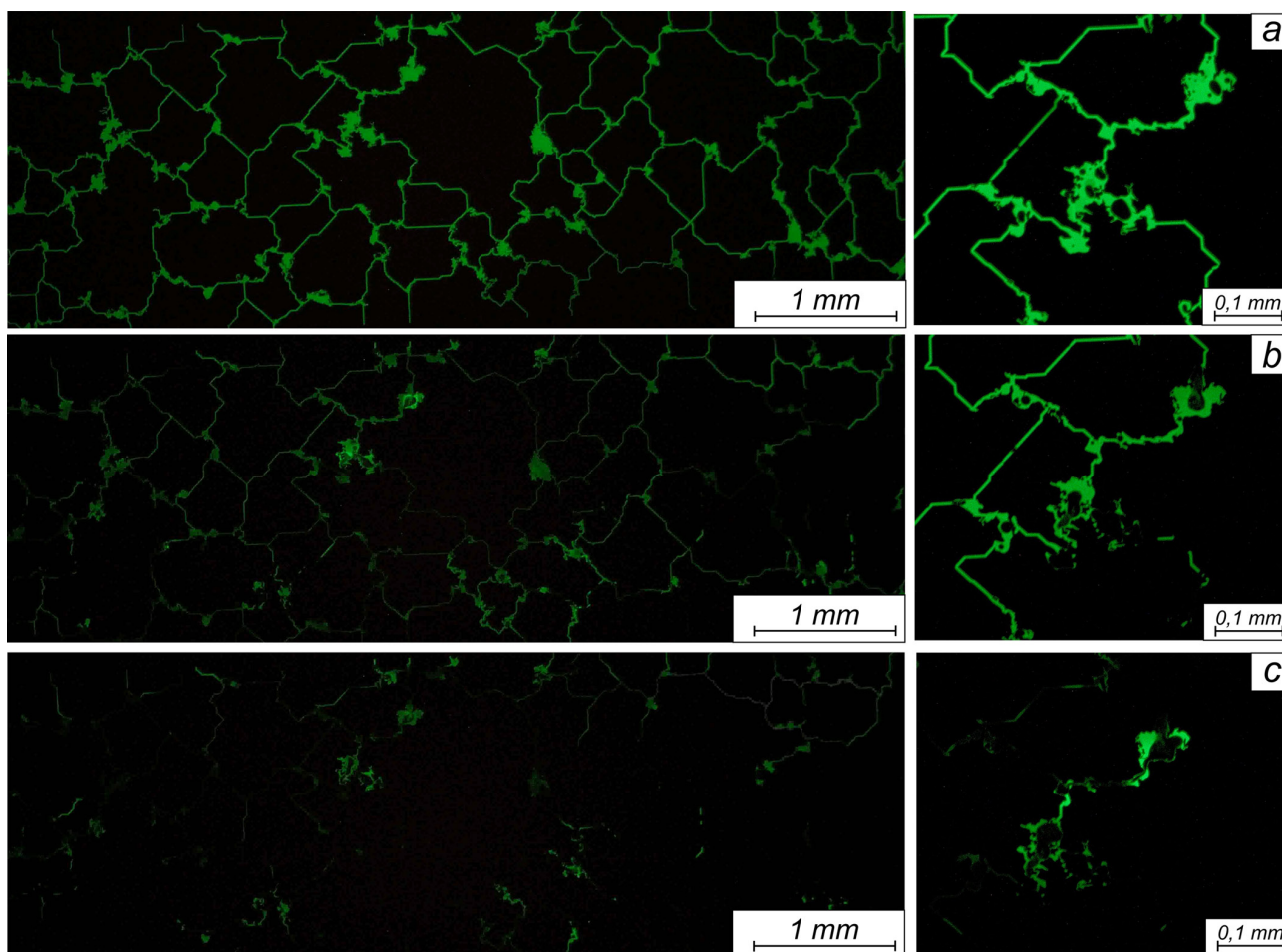
www.geors.ru

Fig. 12. Photos of microfluidic chip porous structure at various stages of fluid injection into the chip to create heterogeneous wettability (a – filling with fluorescent reservoir water; b – water replacement with a hydrophobizer; c – macroporosity is completely filled with acid, formation water remains in micropores)

including: (1) permeability; (2) pore size distribution; (3) average channel diameter; (4) channel tortuosity; (5) macro-to-micro porosity ratio; and (6) pore geometry. The microporosity in this model is reconstructed as a fine mesh (cell size in the mesh is 0.8 µm).

2. Using this new methodology, three artificial porous models were designed that closely replicate the key characteristics of the pore space as determined through digital core modeling. This new method is suitable for the accurate generation of low-permeability structures, which are technically challenging to model.

3. Studied Achimov sandstones are represented by well-sorted, fine-to-medium-grained polymictic arkoses. No significant correlation between permeability and the mineralogical composition of the samples was observed; however, samples with a slightly higher amount of secondary carbonate cement predictably exhibit lower permeability values. Thus, it was demonstrated that the relationship between the mineralogical composition of the samples and their pore space characteristics is not straightforward. Likely, the only parameter that

significantly affects rock permeability is secondary calcitization.

4. A complex of lithological and mineralogical methods enabled the identification of minerals associated with macro- and micropores. It was found that the primary structure of the pore space was disrupted due to late diagenetic processes. Macro-pores in the studied sandstones mainly formed due to the leaching of feldspars, while microporosity is more closely related to the structure of clay minerals, which fill the intergranular space.

5. A methodology for modifying wettability within artificially designed porous structures in a microfluidic chip was developed. This method allows the replication of heterogeneous wettability, which is characteristic of low-permeability sandstones in gas-condensate reservoirs. The developed method enables the retention of hydrophilic micropores within the porous structure, while macro-pores become more hydrophobic due to the reaction between the silicon substrate of the microfluidic chip and the hydrophobizing agent.

6. The comprehensive research conducted on real samples will allow the extrapolation of coreflooding test results to rocks with similar mineralogical characteristics and pore space properties in the future.

Thus, this work represents the first application of an integrated approach for replicating the porous structure of core samples in a silicon microfluidic chip, which included: CT imaging of the core, lithological description of petrographic thin sections, X-ray diffraction analysis, scanning electron microscopy, and contact angle measurements of wettability. This comprehensive approach of solving the problem provides the most reliable results and will enable a quality interpretation of the conducted coreflooding tests in the future.

Acknowledgements

References

Ali M., Jha N. K. Al-Yaseri A., Zhang Y., Iglauer S., Sarmadivaleh M. (2021). Hydrogen wettability of quartz substrates exposed to organic acids; Implications for hydrogen geo-storage in sandstone reservoirs. *Journal of Petroleum Science and Engineering*, 207, 109081. https://doi.org/10.1016/j.petrol.2021.109081

Amott E. (1959). Observations Relating to the Wettability of Porous Rock. *Trans*, 216, pp. 156–162. https://doi.org/10.2118/1167-G

Bartell F.E., Osterhof J.J. 1927. Determination of the Wettability of a Solid by a Liquid. *Ind. Eng. Chem.*, 19(11), pp. 1277–1280.

Bera B., Mitra S.K., Vick D. (2011). Understanding the micro structure of Berea Sandstone by the simultaneous use of micro-computed tomography (micro-CT) and focused ion beam-scanning electron microscopy (FIB-SEM). *Micron*, 42(5), pp. 412–418. doi: 10.1016/j.micron.2010.12.002

Bera B., Gunda N.S.K., Mitra S.K., Vick D. (2012). Characterization of Nanometer-Scale Porosity in Reservoir Carbonate Rock by Focused Ion Beam–Scanning Electron Microscopy. *Microscopy and Microanalysis*, 18(01), pp. 171–178. doi: 10.1017/s1431927611012505

Beucher S., Lantuejoul C. (1979). Use of watersheds in contour detection. International Workshop on Image Processing, Rennes, France, pp. 2.1–2.12.

Beucher, S. (1991). The watershed transformation applied to image segmentation. *Conference on Signal and Image Processing in Microscopy and Microanalysis*, Cambridge, UK, pp. 299–314.

Beucher S., Meyer F. (1993). The morphological approach to segmentation: the watershed transformation. *Mathematical Morphology in Image Processing*, 12, pp. 433–481.

Bobek J.E., Mattax C.C., Denekas M.O. (1958). Reservoir rock wettability-its significance and evaluation. *Transactions of the AIME*, 213(1), pp. 155–160. https://doi.org/10.2118/895-G

Buchgraber M., Clemens T., Castanier L.M., Kovscek A.R. (2011). A Microvisual Study of the Displacement of Viscous Oil by Polymer Solutions. *SPE Reserv Eval Eng.*, 14(03), pp. 269–280.

Decision of the 5th Interdepartmental Regional Stratigraphic Meeting on Mesozoic Deposits of the West Siberian Plain (1991). Editor: I.I. Nesterov; deputy editors: V.S. Bochkarev, Y.V. Braduchan; editors: N.A. Belousova, V.I. Ilyina, A.M. Kazakov et al. Tyumen: ZapSib-NIIGNI, 54 p. (In Russ.)

Dorhjie, D.B., Pereponov, D., Aminev, T., Gimazov, A., Khamidullin, D., Kuporosov, D., Tarkhov, M., Rykov, A., Filippov, I., Mukhina, E. and Shilov, E. (2024). A Microfluidic and Numerical Analysis of Non-equilibrium Phase Behavior of Gas Condensates. *Scientific Reports*, 14(1), p. 9500. https://doi.org/10.1038/s41598-024-59972-x

Gunde A.C., Bera B., Mitra S.K. (2010). Investigation of water and CO2 (carbon dioxide) flooding using micro-CT (micro-computed tomography) images of Berea sandstone core using finite element simulations. *Energy*, 35(12), pp. 5209–5216. doi:10.1016/j.energy.2010.07.045

Gunde K.N.S., Bera B., Karadimitriou N.K., Mitra S.K., Hassanizadeh S.M. (2011). Reservoir-on-a-Chip (ROC): A new paradigm in reservoir engineering. *Lab on a Chip*, 11(22), pp. 3785–3792. https://doi.org/10.1039/C1LC20556K

Iglauer S., Ali M., Keshavarz A. (2021). Hydrogen wettability of sandstone reservoirs: Implications for hydrogen geo-storage. *Geophysical Research Letters*, 48(5). https://doi.org/10.1029/2020GL090814

Johansen R.T., Dunning H.N. (1961). Relative wetting tendencies of crude oils by capillarimetric method. US Department of the Interior, *Bureau of Mines*, 5752.

Karadimitriou N.K. (2013). Two-phase flow experimental studies in micro-models. Utrecht Studies in Earth Sciences, 34 (Dissertation) 211 p.

Koh K.S., Chin J., China J., Chiang C.L. (2012). Quantitative Studies on PDMS-PDMS Interface Bonding with Piranha Solution and its Swelling Effect. Micromachines, 3, pp. 427–441. doi: 10.3390/mi3020427

Kurchikov A.R., Borodkin V.N., Nedosekin A.S., Zaboev K.O., Galinsky K.A. (2013). Lithological characteristics, reservoir properties and oil and gas bearing capacity of Lower Cretaceous sediments of the Nerutinskaya Depression and adjacent territories in the north of Western Siberia. *Geology, Geophysics and Development of Oil and Gas Fields*, 7, pp. 4–13. (In Russ.)

Kuznetsov, M.A., Ishkinov, S.M., Kuznetsova, T.I., Fakhretdinov, R.N., Yakimenko, G.H., Sidorov, R.V., Bobylev, O.A. (2017). Technology of limiting water inflows into producing wells. *Petroleum Engineering. Development and exploitation of oil fields*, 7, pp. 58–60. (In Russ.)

Lacey M., Hollis C., Oostrom M., Shokri N. (2017). Effects of Pore and Grain Size on Water and Polymer Flooding in Micromodels. *Energy and Fuels*, 31(9), pp. 9026–9034. https://doi.org/10.1021/acs.energyfuels.7b01254

Lei W., Lu X., Liu F., Wang M. (2022). Non-monotonic wettability effects on displacement in heterogeneous porous media. *J. Fluid Mech*, (942 R5), https://doi.org/10.1017/jfm.2022.386

Li T., Li Y., Zhang F., Liang N., Yin J., Zhao H., Yang Y., Chen B., Yang L. (2023). Piranha Solution-Assisted Surface Engineering Enables Silicon Nanocrystals with Superior Wettability and Lithium Storage. *Crystals*, 13(7), 1127. https://doi.org/10.3390/cryst13071127

Lifton V.A. (2016). Microfluidics: an enabling screening technology for enhanced oil recovery (EOR). Lab on a Chip. *Royal Society of Chemistry*, pp. 1777–1796. https://doi.org/10.1039/C6LC00318D

Mittal K.L. (2004). Contact Angle, Wettability and Adhesion, 3. CRC Press., 520 p.

Mooney R.W., Keenan A.G., Wood L.A. (1952). Adsorption of water vapor by montmorillonite. II. Effect of exchangeable ions and lattice swelling as measured by X-ray diffraction. *Journal of the American Chemical Society*, 74(6), pp. 1371–1374.

Moore, T.F., Slobod R.L. (1955). Displacement of Oil by Water-Effect of Wettability, Rate, and Viscosity on Recovery. Paper presented at the Fall *Meeting of the Petroleum Branch of AIME*, New Orleans, Louisiana, October, SPE-502-G. https://doi.org/10.2118/502-G

Repetition of the void space structure of Achimov sandstones…   M.R. Latypova, D.I. Pereponov, V.V. Kazaku et al.

gr

www.geors.ru

Morris K.A., Shepperd C.M. (1982) The role of clay minerals in influencing porosity and permeability characteristics in the Bridport Sands of Wytch Farm, Dorset. *Clay Minerals*, 17(1), pp. 41–54. https://doi.org/10.1180/claymin.1982.017.1.05

Mungan N. (1972). Relative permeability measurements using reservoir fluids. *Society of Petroleum Engineers Journal*, 12(5), pp. 398–402. https://doi.org/10.2118/3427-PA

Nelson P.H. (2009). Pore-throat sizes in sandstones, tight sandstones, and shales. *AAPG Bull*, 93, pp. 329–340. https://doi.org/10.1306/10240808059

Panikarovsky E.V., Panikarovsky V.V., Mansurova M.M., Listak M.V. (2020). Application of multistage hydraulic fracturing in the development of Achimov deposits of the Urengoyskoye field. *Oil and Gas Studies*, 2, pp. 38–48. (In Russ.) https://doi.org/10.31660/0445-0108-2020-2-38-48

Pereponov D., Tarkhov M., Dorhjie D.B., Rykov A., Filippov I., Zenova E., Krutko V., Cheremisin A., Shilov E. (2023). Microfluidic Studies on Minimum Miscibility Pressure for n-Decane and CO2. *Energies*, 16, 4994. https://doi.org/10.3390/en16134994

Pradhan S., Shaik I., Lagraauw R., Bikkina P. (2019). A semi-experimental procedure for the estimation of permeability of microfluidic pore network. MethodoX, 6, pp. 706–713. https://doi.org/10.1016/j.mex.2019.03.025

Romm E.S. (1985). Structural models of rock pore space. Leningrad: Nedra, 240 p. (In Russ.)

Rushing J. A., Newsham K. E., Blasingame T. A. (2008). Rock typing—Keys to understanding productivity in tight gas sands. *SPE Unconventional Resources Conference*. Gas Technology Symposium, 114164. SPE-114164-MS. https://doi.org/10.2118/114164-MS

Salathiel R. (1973). A. Oil recovery by surface film drainage in mixed-wettability rocks. *Journal of petroleum technology*, 25(10), pp. 1216–1224. https://doi.org/10.2118/4104-PA

Scerbacova A., Pereponov D., Tarkhov, M., Kazaku, V., Rykov A., Filippov I., Zenova E., Krutko V., Cheremisin A., Evgeny S. (2023). Visualization of Surfactant Flooding in Tight Reservoir Using Microfluidics. *Paper presented at the SPE - Europe Energy Conference featured at the 84th EAGE Annual Conference & Exhibition*, Vienna, Austria. https://doi.org/10.2118/214419-MS

Scherer M. (1987). Parameters Influencing Porosity in Sandstones: A Model for Sandstone Porosity Prediction. *AAPG bulletin*, 71(5), pp. 485–491. https://doi.org/10.1306/94886ED9-1704-11D7-8645000102C1865D

Slobod R.L., Blum H.A. (1952). Method for Determining Wettability of Reservoir Rocks. *J Pet Technol*, 4 (1952), pp. 1–4. doi: https://doi.org/10.2118/137-G

Strassner J. E. (1968). Effect of pH on interfacial films and stability of crude oil-water emulsions. *Journal of Petroleum Technology*, 20(3), pp. 303–312. https://doi.org/10.2118/1939-PA

Xi K., Cao Y.C., Jahren J., Zhu R.K., Bjorlykke K., Haile B.G., Zheng L.J., Hellevang H. (2015). Diagenesis and reservoir quality of the lower cretaceous quantou formation tight sandstones in the southern Songliao Basin, China. *Sedimentary Geology*, 330, pp. 90–107. https://doi.org/10.1016/j.sedgeo.2015.10.007

Zahiri B., Sow P. K., Kung C.H., Merida W. (2017). Active Control over the Wettability from Superhydrophobic to Superhydrophilic by Electrochemically Altering the Oxidation State in a Low Voltage Range. *Advanced Materials Interfaces*, 1700121. https://doi.org/10.1002/admi.201700121

About the Authors

Margarita R. Latypova – PhD (Geology and Mineralogy), LABADVANCE LLC; postgraduate student, engineer of the I category of the Department of Regional Geology and Earth History, Faculty of Geology, Lomonosov Moscow State University

11 Sikorsky st., Skolkovo Innovation Centre, Moscow, 121205, Russian Federation

1 Leninskie Gory, Moscow, 119234, Russian Federation

e-mail: latypova@labadvance.net

Dmitrii I. Pereponov – Postgraduate student, Skolkovo Institute of Science and Technology; Research scientist, LABADVANCE LLC

Build. 1, 30 Bolshoi Boulevard, Skolkovo Innovation Centre, Moscow, 121205, Russian Federation

e-mail: dmitrii.pereponov@skoltech.ru

Vitaly V. Kazaku – Postgraduate student, Skolkovo Institute of Science and Technology; Research scientist, LABADVANCE LLC

Build. 1, 30 Bolshoi Boulevard, Skolkovo Innovation Centre, Moscow, 121205, Russian Federation

e-mail: kazaku@labadvance.net

Alexandra Scerbacova – PhD (Technical Sciences), Postdoc researcher at Sustainable and Resilient Materials Lab, Center for Integrative Petroleum Research, College of Petroleum Engineering & Geosciences, King Fahd University of Petroleum and Minerals

Saudi Arabia, 31261, Dhahran

e-mail: alexandra.scerbacova@kfupm.edu.sa

Igor G. Maryasev – Head of the geological research sector, Systems for Microscopy and Analysis LLC

Office 45, 20 Skolkovskoe shosse, Moscow, 121353, Russian Federation

e-mail: maryasev@microscop.ru

Roman A. Mukhin – Research scientist, Systems for Microscopy and Analysis LLC

Office 45, 20 Skolkovskoe shosse, Moscow, 121353, Russian Federation

e-mail: mukhin@microscop.ru

Evgeny D. Shilov – Research assistant, Skolkovo Institute of Science and Technology; Technical Director, LABADVANCE LLC

Build. 1, 30 Bolshoi Boulevard, Skolkovo Innovation Centre, Moscow, 121205, Russian Federation

e-mail: shilov@labadvance.net

Alexey N. Cheremisin – PhD (Technical Sciences), Professor, Deputy Director for Experimental Research of the Centre for Oil and Gas Science and Engineering (Skoltech Petroleum), General Director, LABADVANCE LLC

Build. 1, 30 Bolshoi Boulevard, Skolkovo Innovation Centre, Moscow, 121205, Russian Federation

e-mail: cheremisin@labadvance.net

Vladimir L. Kosorukov – Senior Lecturer of the Department of Oil and Gas Sedimentology and Marine Geology, Faculty of Geology, Lomonosov Moscow State University

1 Leninskie Gory, Moscow, 119234, Russian Federation

e-mail: kosorukov-vladimir@rambler.ru

Valeria V. Churkina – Leading engineer of the Department of Geology and Geochemistry of Combustible Fossils, Faculty of Geology, Lomonosov Moscow State University

1 Leninskie Gory, Moscow, 119234, Russian Federation

e-mail: Lera.keily@gmail.com

Mikhail A. Tarkhov – PhD (Physical and Mathematical Sciences), Head of the Research Laboratory of Quantum Technologies (RLQ), Institute of Nanotechnologies of Microelectronics of the Russian Academy of Sciences

32A Leninsky ave., Moscow, 119334, Russian Federation

e-mail: tmafuz@mail.ru

Vladimir A. Shtinov – Head of Hydrodynamic Modelling Department, RN-BashNIPIneft LLC

Build. 1, 86 Lenina st., Ufa, 450006, Russian Federation

e-mail: ShtinovVA@bnipi.rosneft.ru

Timur E. Nigmatullin – Head of Well Workover Technologies Department, RN-BashNIPIneft LLC

Build. 1, 86 Lenina st., Ufa, 450006, Russian Federation

e-mail: NigmatullinTE@bnipi.rosneft.ru

Eduard S. Batyrshin – Head of Innovative Research Laboratory, RN-BashNIPIneft LLC

Build. 1, 86 Lenina st., Ufa, 450006, Russian Federation

e-mail: BatyrshinES@bnipi.rosneft.ru

Igor V. Samsonov – Head of Special Research Department, Field Development Department, ROSPAN INTERNATIONAL JSC

26/1 Sofiyskaya emb., Moscow, 117997, Russian Federation

e-mail: IV_Samsonov2@rspn.rosneft.ru

Repetition of the void space structure of Achimov sandstones…   M.R. Latypova, D.I. Pereponov, V.V. Kazaku et al.

gr

www.geors.ru

IN RUSSIAN

Воспроизведение структуры пустотного пространства ачимовских песчаников Восточно-Уренгойского месторождения в искусственно созданной геометрии кремниевого микрофлюидного чипа

М.Р. Латыпова[1,2*], Д.И. Перепонов[1,3], В.В. Казаку[1,3], А. Щербакова[4], И.Г. Марясев[5], Р.А. Мухин[5], Е.Д. Шилов[1,3], А.Н. Черемисин[1,3], В.Л. Косоруков[2], В.В. Чуркина[2], М.А. Тархов[6], В.А. Штинов[7], Т.Э. Нигматуллин[7], Э.С. Батыршин[7], И.В. Самсонов[8]

[1]ООО «ЛАБАДВАНС», Москва, Россия
[2]Московский государственный университет им. М.В. Ломоносова, Москва, Россия
[3]Сколковский институт науки и технологий, Москва, Россия
[4]Университет нефти и минералов им. короля Фахда, Дахран, Саудовская Аравия
[5]ООО «Системы для микроскопии и анализа», Москва, Россия
[6]Институт нанотехнологий микроэлектроники РАН, Москва, Россия
[7]ООО «РН-БашНИПИнефть», Уфа, Россия
[8]АО «РОСПАН ИНТЕРНЕШНЛ», Новый Уренгой, Россия

Разработана уникальная методика воспроизведения структуры пустотного пространства низкопроницаемого коллектора в кремниевом микрофлюидном чипе, которая обеспечивает повторяемость ключевых параметров структуры пустотного пространства: проницаемость; распределение пор по размеру; средний диаметр каналов; извилистость каналов, соотношение макро- к микропористости по данным цифрового керна. Разработанная методика позволяет в точности копировать геометрию пор образца керна с микротомографических снимков и воссоздавать ее внутри микрофлюидного чипа.

По данной схеме разработаны искусственные структуры пустотного пространства для трех образцов ачимовских песчаников различной проницаемости. Проведенный расширенный комплекс геолого-минералогических исследований на этих образцах позволит распространить результаты будущих фильтрационных тестов на породы со схожими минералогическими характеристиками и фильтрационно-емкостными свойствами.

С целью воссоздания структуры неоднородной смачиваемости реальной горной породы в кремниево-боросиликатном микрофлюидном чипе разработан качественно новый метод частичной гидрофобизации искусственно созданного пустотного пространства в микрочипе, который заключается в плавном вытеснении пластовой воды из структуры чипа гидрофобизатором.

В настоящей работе впервые применен комплексный многопрофильный подход для воспроизведения структуры пустотного пространства керна внутри микрофлюидного чипа. В будущем данная методика будет совершенствоваться, чтобы результаты фильтрационных тестов на микрофлюидных чипах еще более достоверно отражали движение флюидов внутри пласта.

Ключевые слова: микрофлюидный чип, низкопроницаемый коллектор, ачимовский клиноформенный комплекс, фильтрационно-емкостные свойства, искусственно созданная структура пустотного пространства, цифровой керн, литолого-минералогический комплекс исследований, неоднородная смачиваемость, модификация смачиваемости